

University of Nebraska - Lincoln
DigitalCommons@University of Nebraska - Lincoln

Biological Systems Engineering: Papers and
Publications

Biological Systems Engineering

2018

Evaluation of variable rate irrigation using a remote-sensing-based model

John Burdette Barker

University of Nebraska-Lincoln, burdette.barker@huskers.unl.edu

Derek M. Heeren

University of Nebraska-Lincoln, derek.heeren@unl.edu


Christopher M.U. Neale

University of Nebraska-Lincoln, cneale@nebraska.edu

Daran Rudnick

University of Nebraska - Lincoln, darán.rudnick@unl.edu

Follow this and additional works at: <https://digitalcommons.unl.edu/biosysengfacpub>

 Part of the [Bioresource and Agricultural Engineering Commons](#), [Environmental Engineering Commons](#), [Hydraulic Engineering Commons](#), and the [Other Civil and Environmental Engineering Commons](#)

Barker, John Burdette; Heeren, Derek M.; Neale, Christopher M.U.; and Rudnick, Daran, "Evaluation of variable rate irrigation using a remote-sensing-based model" (2018). *Biological Systems Engineering: Papers and Publications*. 525.

<https://digitalcommons.unl.edu/biosysengfacpub/525>

This Article is brought to you for free and open access by the Biological Systems Engineering at DigitalCommons@University of Nebraska - Lincoln. It has been accepted for inclusion in Biological Systems Engineering: Papers and Publications by an authorized administrator of DigitalCommons@University of Nebraska - Lincoln.

Published in *Agricultural Water Management* 203 (2018), pp 63–74.

doi 10.1016/j.agwat.2018.02.022

Copyright © 2018 Elsevier B.V. Used by permission.

Submitted 1 June 2017; revised 15 February 2018; accepted 19 February 2018;

published 08 March 2018.

Evaluation of variable rate irrigation using a remote-sensing-based model

J. Burdette Barker,¹ Derek M. Heeren,²
Christopher M.U. Neale,³ and Daran R. Rudnick⁴

1 Biological Systems Engineering Department, University of Nebraska-Lincoln, 153 L.W. Chase Hall, 3605 Fair St., Lincoln, NE, 68583-0726, United States

2 Biological Systems Engineering Department, University of Nebraska-Lincoln, and Robert B. Daugherty Water for Food Global Institute at the University of Nebraska Faculty Fellow, 241 L.W. Chase Hall, 3605 Fair St., Lincoln, NE, 68583-0726, United States

3 Robert B. Daugherty Water for Food Global Institute at the University of Nebraska, Biological Systems Engineering Department, University of Nebraska-Lincoln, 2021 Transformation Dr., Suite 3220, Lincoln, NE, 68588-6203, United States

4 West Central Research and Extension Center, University of Nebraska-Lincoln, and Robert B. Daugherty Water for Food Global Institute at the University of Nebraska Faculty Fellow, 402 W. State Farm Road, North Platte, NE, 69101-7751, United States

Corresponding author — D. M. Heeren, derek.heeren@unl.edu

E-mail addresses — J. B. Barker, burdette.barker@huskers.unl.edu;

C.M.U. Neale, cneale@nebraska.edu; D. R. Rudnick, daran.rudnick@unl.edu

Abstract

Improvements in soil water balance modeling can be beneficial for optimizing irrigation management to account for spatial variability in soil properties and evapotranspiration (ET). A remote-sensing-based ET and water balance model was tested for irrigation management in an experiment at two University of Nebraska-Lincoln research sites located near Mead and Brule, Nebraska. Both fields included a center pivot equipped with variable rate irrigation (VRI). The study included maize in 2015 and 2016 and soybean in 2016 at Mead, and maize in 2016 at Brule, for a total of 210 plot-years. Four irrigation treatments were applied at Mead, including: VRI based on a remote sensing model (VRI-RS); VRI based on neutron probe soil water content measurement (VRINP); uniform irrigation based on neutron probe measurement; and rainfed. Only the VRI-RS and uniform treatments were applied at Brule. Landsat 7 and 8 imagery were used for model input. In 2015, the remote sensing model included reflectance-based crop coefficients for ET estimation in the water balance. In 2016, a hybrid component of the model was activated, which included energy-balance-modeled ET as an input. Both 2015 and 2016 had above-average

precipitation at Mead; subsequently, irrigation amounts were relatively low. Seasonal irrigation was greatest for the VRI-RS treatment in all cases because of drift in the water balance model. This was likely caused by excessive soil evaporation estimates. Irrigation application for the VRI-NP at Mead was about 0 mm, 6 mm, and -12 mm less in separate analyses than for the uniform treatment. Irrigation for the VRIRS was about 40 mm, 50 mm, and -98 mm greater in separate analyses than the uniform at Mead and about 18mm greater at Brule. For maize at Mead, treatment effects were primarily limited to hydrologic responses (e.g., ET), with differences in yield generally attributed to random error. Rainfed soybean yields were greater than VRI-RS yields, which may have been related to yield loss from lodging, perhaps due to over-irrigation. Regarding the magnitude of spatial variability in the fields, soil available water capacity generally ranked above ET, precipitation, and yield. Future research should include increased cloud-free imagery frequency, incorporation of soil water content measurements into the model, and improved wet soil evaporation and drainage estimates.

Keywords: Evapotranspiration, Remote sensing, Soil water balance, Variable rate irrigation

1. Introduction

Modeled water balances are a common method for irrigation management (e.g., Martin et al., 1990). Irrigation management may be improved by using spatial evapotranspiration (ET) and soil water models. A number of spatial ET models have been developed and tested for this purpose (Gowda et al., 2007). While useful in general, spatial ET may be of particular interest in variable rate irrigation (VRI) management.

In previous research, Lo et al. (2016) quantified reductions in pumping from using VRI to manage for spatial variability in available water capacity (AWC) but did not account for spatial variability in ET. Accurate subfield-scale ET and water balance models could provide a valuable spatial component to VRI and conventional irrigation application. Stone et al. (2016) used a multispectral remote-sensing-based ET model for VRI management with promising results. However, there is a need for VRI research performed at the scale of commercial production fields (e.g. 60 ha).

One benefit of applying remote-sensing-based models in irrigation management is that such models include an indirect, spatial measurement of the integrated crop response. When coupled with spatial soil property data, remote sensing ET models may be used to compute spatial soil water balances (e.g. Neale et al., 2012). These models have potential to be used for spatially informed irrigation management. Furthermore, monitoring soil water alone is likely to be an impractical solution

for VRI management; Barker et al. (2017) determined that three monitoring locations would be needed per management zone if using a neutron probe for their study conditions. The hybrid model of Neale et al. (2012) is one such ET and water balance model that is suited for irrigation management. (Barker et al., 2018) refined this hybrid model and evaluated its potential for use in VRI management. The hybrid model is a combination of reflectance-based crop coefficients (K_{cbrf} ; Bausch and Neale, 1987; Neale et al., 1989) and the two-source energy balance model (TSEB) of Norman et al. (1995). The K_{cbrf} method follows the reference ET (ET_r) approach of estimating crop ET (ET_c), employing a dimensionless crop coefficient (K_c) as:

$$ET_c = ET_r K_c = ET_r (K_s K_{cb} + K_e) \quad (1)$$

where K_s , K_{cb} , and K_e are dimensionless water stress, basal, and evaporation coefficients, respectively (Allen et al., 1998; Jensen and Allen, 2016; Wright, 1982). A water balance model may be used to compute K_s and K_e as presented by Allen et al. (1998). The K_{cb} relates to the vegetation's potential to transpire and may change with crop, time, and location (Allen et al., 1998; Wright, 1982). We refer to ET_c computed using K_{cbrf} as ET_{crf} in the remainder of this article.

In the K_{cbrf} method, the K_{cb} is found using relationships between K_{cb} and reflectance-based vegetation indices (Bausch, 1993; Bausch and Neale, 1987). The normalized difference vegetation index (NDVI; e.g. Rouse et al., 1974), may be used for this purpose as in Neale et al. (1989). Bausch (1993) used the soil adjusted vegetation index (SAVI; Huete, 1988) for this purpose. A water balance can then be computed to model the soil water status of the managed crop root zone (Allen et al., 1998; Martin et al., 1990). One approach may be to compute the water balance following the United Nations' Food and Agricultural Organization's Irrigation and Drainage Paper No. 56 (Allen et al., 1998), hereafter referred to as FAO56. Such an approach was applied by Stone et al. (2016).

In the hybrid methodology, Neale et al. (2012) used the K_{cbrf} method with a water balance to model soil water depletion. The benefit of the hybrid method was that a K_{cbrf} is relatively easy to estimate for periods between multispectral image collection dates (Barker et al., 2018; Neale et al., 2012). Thus, ET may be modeled even on days without remote sensing imagery. On thermal infrared image acquisition dates, the model of Neale et al. (2012) also incorporates a second estimate of ET using the TSEB, which is separate from the modeled water balance (Barker et al., 2018). The TSEB is a surface energy balance method, which partitions

remotely-sensed radiometric temperature of the land surface into crop and soil temperatures (Norman et al., 1995). The energy balance is solved for both crop and soil components. A challenge with the TSEB is that it requires thermal infrared imagery, limiting its use to dates of image acquisition (e.g. satellite overpass). Further detail on the TSEB model is provided in Barker et al. (2018).

The TSEB ET is incorporated into the water balance model using statistical interpolation (Neale et al., 2012). The statistical weighting function used by Neale et al. (2012) to incorporate TSEB ET into the model is:

$$ET_{WB}^A = ET_{WB}^B + W (ET_{TSEB} - ET_{WB}^B) \quad (2)$$

where the subscripts WB and TSEB represent ET from the K_{cbrf} -based water balance and ET from the TSEB model, respectively, and the superscripts B and A are before and after incorporation of the TSEB ET, and W is the Kalman gain (Barker et al., 2018; Neale et al., 2012). Upon incorporation of the TSEB ET, the water balance is updated by backcalculating the root zone depletion that would produce the K_s necessary to compute ET_{WB}^A (Eq. (2); Barker et al., 2018; Geli, 2012). Thus, the hybrid method should be less prone to large water balance drift compared to modeling ET with only a K_{cbrf} -based water balance.

Other studies have tested the hybrid method (e.g., Barker et al., 2018; Neale et al., 2012). To adopt the method for irrigation management, including VRI, there remains a need to test the methodology in irrigation scheduling. Therefore, the main objective of the present study was to determine whether managing VRI at a production scale using the hybrid model (Neale et al., 2012) would result in reduced irrigation application without yield reduction, or at least result in improved irrigation water use efficiency (see Howell, 2001). This was done by using a remote-sensing-based water balance model to manage irrigation in a field experiment along with other irrigation treatments. The spatial variability of AWC, ET, and yield were also assessed to identify the importance of each in spatial irrigation management.

2. Materials and methods

2.1. Study sites

A remote-sensing-based water balance model was tested for VRI management in 2015 and 2016 at two field sites. The primary study site was

a center pivot irrigated field (41.165°N, 96.430°W, source: Google Earth) at the University of Nebraska-Lincoln's Eastern Nebraska Research and Extension Center located near Mead, Nebraska (Mead; Fig. 1). The field is approximately 53 ha in cropped area including rainfed corners and an access road, as computed using ArcGIS 10.4 (Esri, Redlands, CA) based on an aerial image from (USDA-FSA, 2012). The soils in the field are primarily silty clay loam and silt loam (Soil Survey Staff, 2016b). The field was managed in roughly north and south halves. The two halves of the field were cropped in opposite maize–soybean annual rotations. The field was managed as no-till using controlled wheel traffic. The only tillage operations were planting and anhydrous ammonia application for maize crops. Otherwise, only minor earthwork had been performed in the field

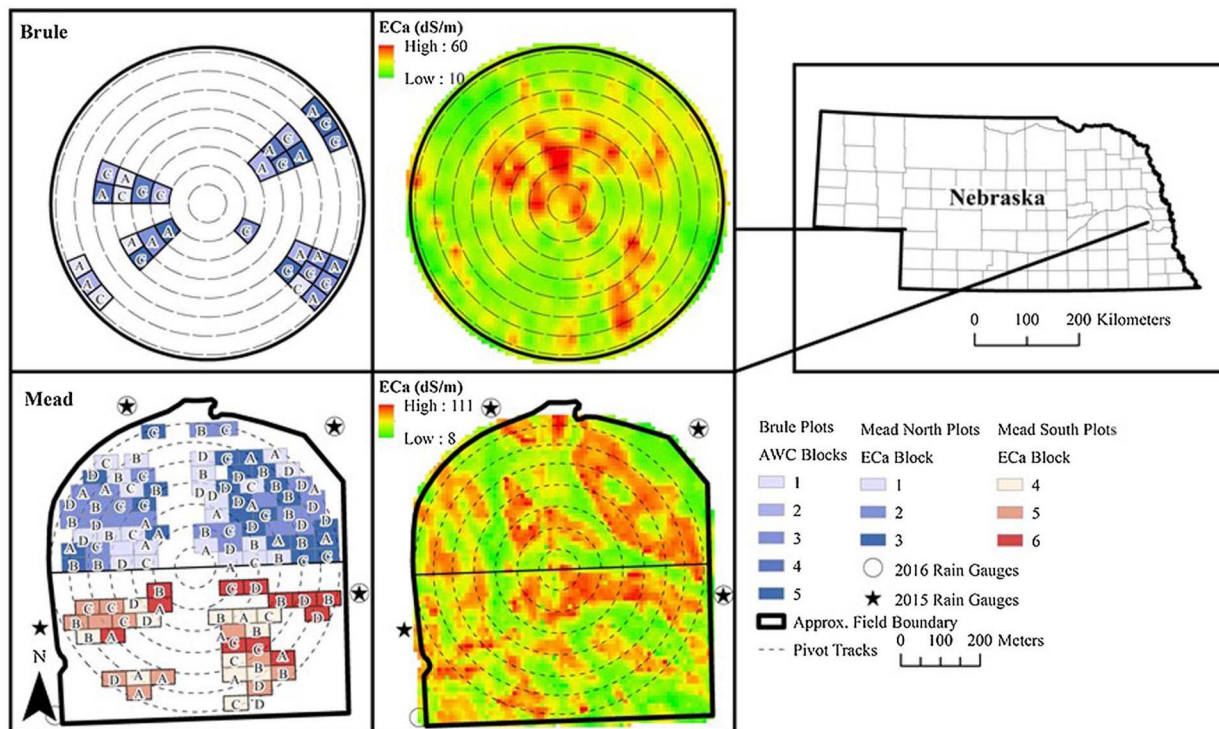


Fig. 1. Site maps for Mead (540mm normal precipitation for May-Oct; NCEI, n.d.) and Brule (308 mm normal precipitation for May-Oct; NCEI, n.d.) fields with plots and EC_a surveys (Brule provided courtesy of Dr. T.E. Franz, UNL; Mead provided by Dr. J. D. Luck, UNL). Treatments were: (A) VRI-RS, (B) VRI-NP, (C) uniform, and (D) rainfed. The EC_a was measured with different equipment and under different conditions at the two sites. Nebraska State map source: USDA-NRCS (2009a), Nebraska county map source: USDA-NRCS (2009b). Mead field boundary based on USDA-FSA (2012). Pivot tower locations and Brule field boundary estimated from pivot sprinkler package documentation provided by the pivot dealers.

Table 1. Agronomic Information for the Study Crops.

<i>Site</i>	<i>Year</i>	<i>Crop</i>	<i>Planting Date</i>	<i>Harvest Date</i>
Mead	2015	Maize	18-May	3-Nov
Mead	2016	Maize	4-May	Oct 31, Nov 1
Mead	2016	Soybean	May 18–19	18-Oct
Brule	2016	Maize	May 12	Oct 25–28

in recent years. The field was grazed with cattle during the winter and at least during the winter between 2015 and 2016 cattle were apparently fed additional forage in parts of the field. Barker et al. (2017) includes further description of the site. The 2015 experiment was implemented in the north half of the field, which was maize. In 2016, the experiment was expanded into the south half to repeat maize, while including soybean in the north half.

A second field (41.029°N, 101.971°W, source: Google Earth) was added in 2016 at the University of Nebraska-Lincoln's West Central Water Resources Field Laboratory, located near Brule, Nebraska (Brule; Fig. 1). The Brule site (approximately 50 ha) was in a drier climate and had greater soil variability than the Mead site. It had alluvial/eolian soils which were primarily loam, loamy sand and gravelly loam (Soil Survey Staff, 2016a). The Brule site was managed as a no-till continuous maize system and was the site of historic residue management research (van Donk et al., 2012). The study plots were in locations within the field that had no residue removal in recent years. **Table 1** provides a list of planting and harvest dates for the study.

Both fields were irrigated with Model 8500 Zimmatic (Lindsay Corporation, Omaha, NE) center pivots. The pivots were equipped with Variable Rate Irrigation options (Lindsay Corporation, Omaha, NE) including individual nozzle control. Sprinklers were mounted on top of the pivot lateral at Mead and on drops roughly 2.1m above ground surface at Brule. The pivot and VRI systems were new in 2014 at Mead and in 2015 at Brule.

2.2. Experimental design

The treatment design was unstructured with four treatments: VRI with remote-sensing-based water balance (VRI-RS), VRI using neutron probe soil water content (VRI-NP), uniform irrigation using neutron probe (uniform), and rainfed. In both VRI treatments, each plot was irrigated according to a plot-specific water balance. In the VRI-RS model, this plot-specific water balance was modeled using remote sensing, without updating the

water balance with soil water content measurements. The VRI-NP treatment was irrigated similarly but used neutron probe measurements to update the water balance and did not include remote sensing input. The uniform treatment was managed similarly to the VRI-NP treatment, but the water balance for only two of the plots was used to manage the entire treatment. The rainfed treatment was prescribed no irrigation. All four treatments were applied in the Mead field. Only the VRI-RS and uniform treatments were included at Brule.

The experimental design at Mead was a generalized randomized complete block design (K.M. Eskridge, personal communication). Plots were blocked into one of three large blocks based on plot median apparent electrical conductivity (EC_a). The median EC_a for each 30.6- by 60.1-m plot was filtered (T. Lo, K.A. Miller and J.D. Luck, personal communications) and interpolated EC_a data from a survey taken on November 12, 2014, using a Veris MSP (Veris Technologies, Salina, KS) (Barker et al., 2017). Deep range EC_a was used as a surrogate for soil texture, specifically clay content (see Sudduth et al., 2005). Three EC_a blocks were generated separately for both the north and south halves of the field using quantiles of median plot EC_a in the respective half. Median plot EC_a was computed without proper regard to geospatial datum differences between interpolated EC_a data and plots, however such should have only minor effect on the blocking assignments. Fig. 1 includes a map of the plot layouts and interpolated EC_a data. The EC_a blocks in the north are labeled 1–3 in Fig. 1 while the blocks in the south are labeled 4–6. In the north half of the field, each treatment was randomly assigned to six plots within each of the EC_a blocks, for a total of 72 plots. The same treatment assignments were maintained in 2015 and 2016. In the south half of the field, only three replicates per block-treatment combination were included for a total of 36 plots.

The Brule field was divided into blocks based on plot AWC (described in 2.4). Quantiles of plot AWC were used to generate five soil blocks. Radial distance from the pivot center was also included as a blocking criterion at Brule to minimize any unexpected effects of the center pivot irrigation system, such as a nozzle getting plugged. Thus the experimental design was a row-column design. The two treatments were randomly assigned to the six radial blocks (pivot spans) and the five AWC blocks, for a total of 30 plots.

At Mead, experimental plots were 36.6m by 60.1m in length along crop rows. Plots were sized to account for a 9.1-m irrigation transition area and to accommodate the yield monitor on the harvest combine (Joe D. Luck, personal communication; Barker et al., 2016). Some areas

of the Mead field were avoided in the plot layout because of: proximity to the pivot center, a buried utility, signs of soil disturbance, historic earthwork (an abandoned railroad), wet/low-yielding area, large within-plot variations in EC_a , and accessibility (Barker et al., 2017). Similar plot dimensions were employed in the Brule field (i.e. minimum plot dimension of 36.6 m). However, other research in that location favored a radial design of the plot layout (Fig. 1). Areas near the center of the field were also excluded at Brule.

Data from some plots were excluded from the final analysis due to herbicide drift, equipment malfunction, etc. The total number of plots included in the analysis at Mead was 66 for 2015 maize, 31 for 2016 maize, and 56 for 2016 soybean. The total number of plots included for maize at Brule in 2016 was 26. Other minor errors were determined to be negligible, see Barker (2017). For example, during irrigation scheduling, a mis-entry of data for the southeast rain gauge at ARDDC for the period June 16–23, 2016, resulted in cumulative precipitation that was 0.8 mm less than it should have been. There were also some rain gauge data entry errors in 2015. Both situations were corrected in post-season processing.

2.3. Experimental satellite, weather, and soil moisture data

Primary experimental data included: remote sensing imagery, weather data, and soil water content measurements. The remote sensing data used in modeling was Landsat 7 and Landsat 8 imagery. Landsat pre-collection data (USGS EROS User Services, personal communication, 9/21/2017) including shortwave surface reflectance data were obtained from the U.S. Geological Survey (USGS; "data available from the U.S. Geological Survey" (<https://lta.cr.usgs.gov/citation>)). Atmospheric corrections for the thermal infrared imagery were applied using surface emissivity values computed following Brunsell and Gillies (2002); see also Barker et al. (2018). A soil emissivity of 0.925 was erroneously used, though a value of 0.955 may have been more appropriate (Brunsell and Gillies, 2002); vegetation emissivity was assumed to be 0.98 (Brunsell and Gillies, 2002). Atmospheric correction parameters were obtained from the online application of Barsi (n.d.) similar to what was detailed by Barker et al. (2018) using input local ground weather data. There was one image for Brule (July 18, 2016) for which correction parameters for the nearest integer latitude and longitude were used because the spatial interpolation of the web application did not work for that date. Thermal infrared image corrections and shortwave image stacking were performed using ERDAS IMAGINE 2014 (Hexagon Geospatial, Madison, AL).

Necessary weather data were obtained from the High Plains Regional Climate Center for the Nebraska Mesonet Memphis 5N and Brule 6SW weather stations for the Mead and Brule sites, respectively. The Memphis 6N weather station is located about 1 km ESE of the Mead field (Google Earth) and the Brule 6SW station is located about 400 m ESE of the Brule field (Google Earth). Instantaneous weather data (for the TSEB) and ET_r were computed from hourly data. ET_r was computed using the ASCE Standardized Tall Reference ET equation (ASCE-EWRI, 2005). Vegetation height near the weather stations was assumed to be about 0.5 m for Mead and 0.2m for Brule ET_r computations. During the experiments, measured wind speed was adjusted for use in ET_r computations in a manner similar to ASCE-EWRI (2005) Eq. B.14c. Wind speed was adjusted for use in the TSEB over the crop canopies assuming an equal friction velocity over the crop and weather station surfaces. Both of these wind adjustment methods may be less accurate (likely resulting in lower estimates of wind speed under some of the study conditions) than the method developed by Allen and Wright (1997). In computing the response variables (see 2.6), the adjustment of Allen and Wright (1997) was used for Mead assuming a 0.5 m crop height and upwind distances of 400 m for both the weather station and reference surfaces. For computing response variables at Brule, the wind was adjusted as in the main report of ASCE-EWRI (2005). Also, an incorrect weather station longitude was used in computing ET_r for Mead during the experiment; this was corrected when computing the response variables. The combined effect of wind adjustment and longitude on annual ET_r in Mead was approximately a 4% increase both years. The effect of the wind adjustment at Brule was an increase of less than 0.2% in annual ET_r .

In addition to the weather station data, four Isco model 674 rain gauges (Teledyne Isco, Lincoln, NE) were installed near the perimeter of the field at the Mead field site (**Fig. 1**). The arithmetic mean precipitation from the four rain gauges was input into the water balance models following approximately weekly downloads. When data from one or more rain gauges was missing or suspect, it was excluded from the arithmetic mean. The Isco rain gauges were calibrated prior to both the 2015 and 2016 seasons. Gauges with unaccepted calibration discrepancies (per the manufacturer's stated accuracy) were adjusted arithmetically; however, this adjustment was only applied in postprocessing for 2015, and the adjustment for 2016 was slightly modified. For the Mead field, the weather station precipitation was only used as needed in real-time irrigation management and for season totals included in 3.2. The Brule 6SW

weather station was the only source of precipitation for the Brule field. Weather station precipitation was taken as-is without time adjustment.

Finally, barometric pressure data for input into the TSEB model was obtained for Mead from the nearby Neb Field 3 COsmic-ray Soil Moisture Observing System (COSMOS) station (Zreda, n.d.; Zreda et al., 2012). For Brule, barometric pressure data were obtained in the form of altimeter settings from the Ogallala AWOS weather station. Barometric pressure was computed using the approximate elevation of the Brule 6SW weather station (HPRCC, 2018) following NWS (n.d.).

In addition to weather and remote-sensing data, volumetric soil water content was monitored for each study plot using neutron probes (Barker et al., 2017). Model 503 Elite Soil Moisture Gauges (CPN International, Concord, CA) were used to monitor soil water content at Mead. Both a Model 503 Elite and a Model 503DR Soil Moisture Gauges (CPN International, Concord, CA) were used at Brule (T. Lo., personal communication). Neutron probe measurements were taken in an approximately 5.1-cm diameter aluminum access tube installed near the center of each plot. At Mead, access tubes were installed roughly midway between the center of the crop row and the center of the interrow. At Brule, tubes were installed in the center of the crop row. Measurements were taken at 15, 30, 46, 76, 107, and 137 cm below ground surface at Mead. Similar depths were used at Brule, omitting the 30-cm reading and including a 168-cm reading. Root-zone-depth-weighted average readings were used to update the water balances for the VRI-NP and uniform treatments. Neutron probe measurements were taken approximately weekly throughout most of the growing season at Mead. The north half of the Mead field was generally monitored in two days (with a couple exceptions). The 2016 maize at Mead was generally monitored in a single day (with a couple exceptions) as was the Brule site. Because of logistical difficulties, neutron probe readings in the late season of 2016 were limited in frequency at both locations.

2.4. Water balance models for irrigation scheduling

Irrigation for the three irrigated treatments was scheduled using computed daily water balances following FAO56 with some deviations. The models were also used for all treatments in computing response variables. In irrigation scheduling for the VRI-NP and uniform treatments, neutron probe data were incorporated into the models as the true daily water status. Details of regarding this process and variation in 2015 are presented in Barker (2017). Such variations also include precipitation and

irrigation incorporation in 2015 (Barker, 2017). Model parameterizations and deviations from the FAO56 methodologies are described below.

Crop ET for the VRI-NP and uniform treatments was modeled using dual crop coefficients as in Eq. (1). In 2015, the K_{cb} followed Allen and Wright (2002). In 2016, the K_{cb} was modified for time scaling in the late season similar to the U.S. Bureau of Reclamation's AgriMet methodology (USBR, 2016). In this methodology, the K_{cb} is scaled based on the fraction of days between planting and effective full cover as in Allen and Wright (2002), but the second portion of the season is scaled based on fraction of time between effective full cover and harvest/termination rather than a set number of days. The corn K_{cb} of Allen and Wright (2002) was used for maize and an adaptation of their dry bean K_{cb} was used for soybean. The primary adjustment to the latter was an extended peak K_{cb} period. Planting dates for the K_{cb} were fixed. However, effective full cover and termination dates were tailored to the crop based on historic SAVI values, crop stage, and other information. For the VRIRS treatment, ET_{crf} was computed as explained in 2.5.

In computing soil evaporation, readily evaporable water (FAO56) was computed using a linear relationship with total evaporable water (FAO56) based on values from Table 19 of FAO56 for a 10 cm evaporation layer depth. In irrigation scheduling, a minimum of readily available water equal to 53% of total available water was erroneously imposed. In the final analysis, a linear relationship based on FAO56 Table 19 to compute readily available water was used and included appropriate adjustment for varying depth of the evaporation layer (FAO56) and upper and lower bounds based on Table 19. The soil evaporation model was initiated at field capacity on one of the first two days of the year, depending on the site-year. Water stress was computed following FAO56; however, no adjustment for ET potential was made in 2015 irrigation scheduling. Zero was used for K_{cb} outside of the growing season in 2015; however, $K_{cb}=0.12$ was used in 2016 and in all cases for the final analyses.

In addition to ET, surface runoff, net irrigation, and deep percolation were also modeled. Runoff was computed using the U.S. Department of Agriculture, Natural Resources Conservation Service runoff equation (USDA-NRCS, 2004), assuming a curve number of 80. Precipitation for each day was treated as a 24-h storm, with a single pulse of precipitation. Net irrigation was computed differently. Prescribed irrigation quantities were assumed to be the actual gross applied irrigation. An application efficiency of 90% was used to compute net infiltrated irrigation. The time of irrigation for each plot was determined from the center pivot travel time, which was computed from irrigation beginning and

ending times (end times were estimated for Brule); speed of travel was assumed to be uniform for a given irrigation cycle. Other non-evaporative subtractions included deep percolation. For irrigation scheduling, deep percolation (DP) for all treatments was computed when the modeled soil water exceeded FC in the 1.2m and 0.9m soil profile for maize and soybean, respectively (FAO56). When neutron probe soil water content was included, if it exceeded FC, DP was not computed until the calculation for the following day in 2015. This allowed some ET to occur from the excess water. In 2016, however, modeled depletion was limited to not be less than zero (a field capacity limit) on the same day as the measurements. The water balance models required both field capacity (FC) and permanent wilting point (WP) for each plot. Plot FC was determined based on neutron probe readings (Lo et al., 2017, who cite Martin et al., 1990). Volumetric soil water content readings from June 30 and July 1, 2015, were used for this purpose for the 2015 season at Mead. Field capacity for the north half of the Mead field was updated in 2016 based on neutron probe readings from May 6, 2016, prior to planting of the soybean crop. The FC values for the south plots at Mead were taken from June 15 and 16, 2016, readings; most depths were read on June 15, but the 30-cm readings were taken on June 16, 2016. For Brule, the June 30, 2016 neutron probe readings were deemed to be an adequate estimate of FC for irrigation scheduling. We recognized that this was likely a low estimate at Brule because it was mid-crop development. For both fields, the weighted-average neutron probe readings down to about 1.2 m were used to compute FC, excluding the 15-cm readings at Mead. The FC used in final analyses ranged from 0.37 to 0.43 $\text{cm}^3 \text{cm}^{-3}$ at Mead and from 0.10 to 0.29 $\text{cm}^3 \text{cm}^{-3}$ at Brule. The ranges of FC used in irrigation scheduling were similar in magnitude, with maxima and minima within $\pm 0.02 \text{ cm}^3 \text{cm}^{-3}$ of those used in final analyses for any of the site-years. In 2016, all water balances were initiated at FC at planting. In 2015, the initial soil water measurement on June 30 and July 1 was used to initiate all water balances.

Plot WP at Mead was based on measurements from soil samples collected in the north half of the field in 2015. Wilting point was measured using a model WP4-T Dewpoint Potential Meter (Decagon Devices, Inc., Pullman, WA). In 2015, an aerial- and depth-averaged WP from samples processed up to that point was used for all plots. Additional WP samples were subsequently processed. A reasonable relationship was computed between profile-averaged WP and deep range EC_a (see 2.2) (Barker, 2017). This was done by pairing each profile WP estimate with a nearby EC_a pixel from the interpolated survey. The accuracy of neutron

probe tube locations was possibly quite low in the roughly east-west direction. The plot WP was computed using mean 10-m EC_a data (resampled to 1-m) within a 9.1-m buffer inside each plot. The resulting relationship was applied to both sides of the field to determine plot-specific WP in 2016 and in final analyses. For the Brule field, WP was determined from measured plot FC and soil survey data. This was done by linear interpolation between the maximum and minimum WP and FC from the soil survey map units (Soil Survey Staff, 2016a). This provided a reasonable estimate of AWC and was justified because the soil textures were coarser than silt loam and thus within the range where FC and WP may have a generally proportional relationship (see Figure 5.29 of Brady and Weil, 1996). Plot WP used in the final analysis ranged from 0.17 to 0.21 $cm^3 cm^{-3}$ at Mead and from 0.05 to 0.15 $cm^3 cm^{-3}$ at Brule. Ranges of WP used in irrigation scheduling were within $\pm 0.02 cm^3 cm^{-3}$ of those used in final analyses for any of the site-years.

During irrigation management, the average FC and WP for all of the plots in a given crop-year were used for the uniform treatment at Mead. Plot-specific FC and WP were used for all plots at Brule because of the increased variability at that site. Plot-specific FC and WP were used for all plots in the final analysis. In irrigation scheduling, root zone total available water (FAO56) was computed using a 1.2-m managed root zone for maize at both sites and a 0.9-m root zone for soybean (Kranz and Specht, 2012). The root zone was assumed to begin at 0.1m and extend linearly to the full managed rooting depth when the K_{cb} reached peak value.

In scheduling irrigation with the water balance models described above, the average daily ET_r from the previous 20 years was used to forecast ET. A management allowable depletion (Merriam, 1966) of 45% was used for maize through most of the season but was increased to 60% near the end of the season (Yonts et al., 2008). In soybean, MAD was set to 55% until around beginning pod, Kranz and Specht (2012) suggest avoiding excess irrigation early in the soybean season. Following this time, MAD was reduced to 50%, which was maintained through the end of the season (Kranz and Specht, 2012). At the end of the season, the modeled root zone was extended to 1.2 m (Yonts et al., 2008).

Irrigation was timed to prevent the water balance from any VRI plot or either of the two plots used for managing the uniform treatment (the average of the two was used before August 2015) from exceeding MAD prior to irrigation. Thus, any of these plots could trigger an irrigation event. Irrigation was applied to achieve a target depth of 38.1 mm of soil water storage above MAD at Mead or 25.4 mm above MAD at Brule. Gross irrigation was limited to be no greater than 30.5 mm per irrigation

at Mead or 25.4 mm at Brule. A minimum limit of 5.1mm per irrigation for any irrigation treatment plot was included at both sites to prevent the supply pumps from operating at undesirably low flow rates. Irrigation management effectively began on July 22, 2015, and July 1, 2016, at Mead and on August 8, 2016, for Brule.

At Brule, prescriptions were computed at the beginning of the week and forecasted to be applied by later in the week. As the treatments were not imposed until August 8, 2016, 187.2 mm of uniform irrigation had been prescribed before treatments began. An additional 50.8 mm of irrigation was prescribed in a "catch-up" mode. The water balances for both treatments for this site showed large estimated soil water deficits. Applying sufficient irrigation to satisfy the experimental protocol seemed unreasonable. It was determined to maintain the scheduling method in place for other research in the study field. Therefore, MAD at Brule was adjusted upward to an achievable irrigation goal each week, based on the magnitude of the measured or modeled soil water depletion. In these adjustments, the same values of MAD were used for both treatments. The MAD values used during this time were quite large, ranging between 75% and 85% of total available water for applied prescriptions. The large soil water depletion at Brule (and increased MAD values) may have been caused in part by: uncertainty in the FC and WP values, possible uncertainty in the neutron probe calibrations, and possible model drift. Additional details regarding the water balance models and the irrigation scheduling are presented in Barker (2017).

2.5. Implementation of the hybrid model

Irrigation prescriptions for the VRI-RS treatment were developed using satellite imagery. The remote-sensing-based water balance followed the approach of Barker et al. (2018) and Barker (2017). The TSEB ET and SAVI calculations were computed using a modified version of the SETMI interface (Barker et al., 2018; Geli and Neale, 2012), which was operated within ArcGIS 10.2 and 10.4 (Esri, Redlands, CA). Plot-level K_{cbrf} and water balance computations were performed in Microsoft Excel. The SETMI computations were performed at either a 0.762-m (the crop row spacing) or a 1-m scale (depending on the site-year). Thus each Landsat 30-m pixel became about 900 to about 1600 smaller pixels of equal value. Plot values of TSEB ET and SAVI were determined by taking the average of the small pixels within each plot excluding a 9.1-m irrigation buffer area within the plot using ArcGIS.

In 2015, only the K_{cbrf} water balance was used for the VRI-RS treatment, and the K_{cbrf} -to-SAVI relationship for maize published by Bausch (1993) was used. This K_{cbrf} relationship was assumed adequate for use with ASCE Standardized (ASCE-EWRI, 2005) tall reference ET_r . To produce daily K_{cb} , we used the maize K_{cb} of Allen and Wright (2002). The K_{cbrf} values were limited to not exceed 0.96 or be less than 0.15 prior to fitting the K_{cb} curves, based on the K_{cb} of Allen and Wright (2002). In 2016, the recently-derived K_{cbrf} relationships of Campos et al. (2017) were used for both soybean and maize crops (Barker et al., 2018). These relationships were developed using eddy covariance flux data from fields near the Mead site (Campos et al., 2017). During irrigation scheduling, the average daily growing degree days from the previous 20 years was used in forecasting. In applying this method, SAVI was limited to not exceed values that produced K_{cbrf} greater than 0.96 for maize at Brule and 0.95 for both crops at Mead, based on the peak K_{cb} for maize and bean in Allen and Wright (2002) and values reported by (Campos et al., 2017). A lower limit on SAVI equivalent to about $K_{cb}=0.12$ was applied in 2016. This lower limit was likely never reached. Forecasted peak and projected end-of-season SAVI values were added as necessary for the soybean in 2016 to improve the K_{cb} until adequate imagery was available (Barker et al., 2018). The projected peak values were for $K_{cb}=0.95$. A similar practice was used at Brule in 2016, employing only the projected end-of-season SAVI. In irrigation scheduling for 2016 maize at Mead, there were too few images available to produce the declining portion of the K_{cb} curve. Therefore, the Allen and Wright (2002) based K_{cb} was used after effective full cover (assumed to occur when the development leg of the K_{cb} curve reached $K_{cb}=0.96$). In irrigation scheduling, K_{cb} was limited to be ≥ 0.15 , and ≤ 0.96 for maize crops and ≤ 0.95 for soybean.

In 2016, the full hybrid model was implemented, including both K_{cbrf} ET and TSEB ET (Barker et al., 2018; Neale et al., 2012). The Penman-Monteith formulation for the TSEB canopy latent heat flux was implemented following Colaizzi et al. (2014). We maintained crop height at the peak value for a given pixel as the modeled vegetation-index-based crop height (Anderson et al., 2004) began to decrease (Barker et al., 2018). Modeled leaf area index (Anderson et al., 2004) was not maintained at peak value after August as in Barker et al. (2018). In coupling the water balance and TSEB models, a Kalman gain (Eq. (2)) of 0.78 was used following Geli (2012).

In implementation of the TSEB, we used the fraction of cover (f_c) equation similar to Li et al. (2005), following the formulation in SETMI (Barker et al., 2018; Geli et al., 2014).

2.6. Response variables and treatment comparisons

The irrigation treatment performance was compared using the following response variables: measurement period actual ET (ET_a), the season ending total precipitation less estimated runoff plus net irrigation plus the change in neutron probe soil water storage ($P-RO+I_{net}+\Delta SW$), estimated deep percolation (DP), and yield. Season total prescribed irrigation was also compared between treatments, but since it was a treatment, it was analyzed separately from the response variables.

The hydrologic response variables were computed together using neutron probe measurements and spreadsheet water balances similar to those used in irrigation scheduling. The measurement periods for Mead were: June 24 and 25 through October 6 and 7, 2015; June 10 to September 26, 2016 for maize; and June 9 and 10 through October 31 and November 1, 2016 for soybean. The computation period for Brule maize was June 23 through November 1, 2016. The water balances were computed similar to the irrigation scheduling water balances for uniform and VRI-NP treatments. However, we used the K_{cbf} methodology discussed by Barker et al. (2018) to run a daily soil water balance (similar to irrigation scheduling for soybean in 2016) and computed fraction of cover from SAVI similar to Barker et al. (2018). We did apply a forecasted peak SAVI, $K_{cbf} \approx 0.95$ for Mead maize in 2016. We effectively did not apply limits to SAVI prior to computing K_{cb} in the final analyses. We similarly did not effectively apply an upper limit on K_{cb} , but did limit $K_{cb} \geq 0.12$. Modeled soil evaporation was also dampened by 25%, based on possible impacts of crop residue (Odhiambo and Irmak, 2012). The surface residue was estimated at two locations in soybean residue on May 18, 2016 using a transect method (Shetlon and Jasa, 2009), with transects perpendicular to the crop rows. The two locations had 46 and 57% residue, respectively. Four locations were measured in the maize residue on about May 13, 2016. Residue at that time ranged from 47 to 70% with an average of 62%. This could represent a reduction in soil evaporation of about 25–30% based on residue alone following FAO56 and Odhiambo and Irmak (2012).

In these calculations, the root zone was maintained at 1.52m for Mead and about 1.22 m at Brule. Brule had a shallower depth because of missing readings in the deeper neutron probe measurements. Measurement period ET_a was estimated from neutron probe measurements and a seasonal water balance ($ET_a = P - RO + I_{net} - DP + \Delta SW$). The seasonal RO only included rainfall events, since runoff from irrigation was already accounted for with the irrigation application efficiency. Runoff

and irrigation were computed as described for irrigation scheduling. We used modeled daily soil water balances to compute DP between neutron probe measurement dates, which were cumulated to get seasonal DP. This method of computing DP was somewhat similar to Irmak et al. (2014) and Djaman and Irmak (2012). The combined variable $P - RO + I_{\text{net}} + \Delta SW$ was computed for the same measurement periods as DP; the combined variable is similar to ET_a but without accounting for DP, eliminating the uncertainty from the method used to compute DP. The combined variable represented a quantity much closer to measurement than did DP and ET_a since we had greater confidence in the measurements and the runoff approximation (see 2.4).

In computing the response variables, the modeled soil water content was allowed to exceed FC for up to three days following the most recent precipitation or irrigation event at Mead and one day at Brule (D.L. Martin, personal communication). That is, the lower constraint of zero root zone depletion was not applied until more than three days had occurred since the last substantial rainfall (resulting in >0 effective precipitation) or irrigation event at Mead and one day at Brule. This change resulted in lower estimates of DP than the DP estimated for irrigation scheduling. This three-day or one-day delay was consistent with the drainage process not being instantaneous. The longer delay at Mead was because of the finer textured soils at that site as compared with the Brule site. In the water balance modeling for response variables, neutron probe measurements were incorporated as the start-of-day soil water depletion for the day following the measurement. No DP was computed on neutron probe measurement dates. All other changes in precipitation, estimated runoff, irrigation, and soil water content were attributed to ET_a . For Brule, revised neutron probe calibrations better suited to the research field were used in ET_a computations. In the final computations at Brule, FC for a given plot and depth was computed as the maximum volumetric water content in all dates discluding neutron probe readings shortly after an irrigation event. The change in FC at Brule also caused a change in WP and AWC; however the original blocking was still honored in the analysis. Field capacity values were also updated for the north half of the field at Mead based on inclusion of a neutron probe standard count that was excluded in FC for 2016 irrigation.

In addition to the hydrologic variables, yield was also estimated. Yield estimates were obtained from the production combines' onboard yield and moisture monitors. Yield maps were processed using the USDA's Yield Editor 2.07 software (Sudduth et al., 2012). Processed yield maps were verified against field total weighing grain cart (N. Thorson, personal

communication) yield at Mead. Yield was similarly processed for Brule, using the yield mass and grain moisture contents provided as output from John Deere APEX software (John Deere, Moline, IL). Yields were reported at harvest moisture content. Final plot yields were obtained by computing the average of all yield points in a plot excluding a 12.2-m buffer inside the plot border. The intent was that all yield points would be within the estimated irrigation transition area of each plot (see Higgins et al., 2016).

Since multiple response variables were included, they were analyzed with multivariate analysis of variance (MANOVA) using PROC GLM in SAS 9.4 (SAS Institute, Inc., Cary, NC). Univariate analyses of variance (ANOVAs) were performed as justified using PROC GLIMMIX in SAS. Type III sums of squares and cross-products were used in all ANOVAs. Blocking was treated as a fixed effect, even though some data were missing. Block-by-treatment interactions were not included in final analysis. Each crop-by-year combination was analyzed separately, rather than as a multi-occasion experiment. We acknowledge that MANOVAs and ANOVAs were used though the response and irrigation data were not tested to see whether they were normally distributed. Seasonal total prescribed irrigation was analyzed separately from the response variables using ANOVA comparing only the two VRI treatments, where possible. The estimated 95% confidence intervals for least-squares means of these two treatments were used to test the null hypothesis that the total prescribed irrigation from each of the VRI treatments was equal to zero (rainfed) or the mean of the uniform treatment. In cases such as Brule maize 2016, where only one VRI treatment was present, a simple mean was computed with standard error and confidence intervals using SAS PROC MEANS.

3. Results and discussion

3.1. Study conditions

The growing seasons at Mead in 2015 and 2016 were wetter than the 1981–2010 normal for the nearby National Weather Service Global Historic Climate Network Mead 6 S station (NCEI, n.d.). The May-to-October precipitation from the rain gauges at the study field (and the Mead Agronomy Farm weather station as needed) was 673 mm in 2015 and 678 mm in 2016. The normal precipitation for May to October for the Mead 6 S station was 540 mm (NCEI, n.d.). Also, 2015 and 2016 were low-ET years with computed May-to-October ET_r of 827 and 932 mm, respectively.

These are compared to 989mm on average for the years 1995–2014, computed using the Mead Agronomy Farm weather station data.

For Brule, the climatic conditions were not similar to Mead. The normal May-to-October precipitation for the Global Historic Climate Network Big Springs weather station near Brule was about 308 mm (NCEI, n.d.). In 2016, the total May-to-October precipitation for the Brule Platte Valley weather station was about 274 mm. Based on the normals (NCEI, n.d.), it is expected that Brule would have substantially more irrigation than Mead. The experiment at Brule was considered to be a proof of concept for operating the model in drier conditions than observed at Mead.

3.2. Satellite imagery

Table 2 provides a list of cloud-free Landsat 7 and Landsat 8 images included in irrigation scheduling and in the final analysis. The low frequency of cloud-free satellite images was a difficulty in this study, particularly at Mead in 2016. The Brule field was in an overlap zone for Landsat images which doubled the frequency of satellite overpasses. Landsat 7

Table 2. Dates of Cloud-Free Landsat Images Included in the Analysis.

<i>Mead Images</i>				<i>Brule Images^a</i>	
<i>Date</i>	<i>Satellite</i>	<i>Crop</i>	<i>TSEB^b</i>	<i>Date</i>	<i>TSEB</i>
Jun 09, 2015	Landsat 8	maize	no	Jun 07, 2016	no
Jul 03, 2015	Landsat 7	maize	no	Jun 16, 2016	yes
Jul 11, 2015	Landsat 8	maize	no	Jun 23, 2016	yes
Aug 12, 2015	Landsat 8	maize	no	Jul 9, 2016	yes
Aug 20, 2015	Landsat 7	maize	no	Jul 18, 2016	yes
Sep 13, 2015	Landsat 8	maize	no	Jul 25, 2016	yes
Sep 29, 2015	Landsat 8	maize	no*	Aug 3, 2016	yes
May 10, 2016	Landsat 8	both	no	Aug 10, 2016	yes
May 26, 2016	Landsat 8	both	no	Sep 11, 2016	yes
Jun 11, 2016	Landsat 8	both	yes	Sep 27, 2016	no*
Jun 27, 2016	Landsat 8	both	yes	Oct 13, 2016	no*
Aug 22, 2016	Landsat 7	soybean	yes	Oct 22, 2016	no*
Sep 23, 2016	Landsat 7	soybean	no*		
Oct 9, 2016	Landsat 7	maize	no*		

a. All images from Brule were Landsat 8, and the only crop was maize.

b. Whether images were used for two-source energy balance (TSEB) evapotranspiration for irrigation scheduling. All images were used in computing reflectance-based crop coefficients in post processing. Those with an * were not included in real-time irrigation management.

images typically did not pick up all of the plots in a single image; therefore, only Landsat 8 was used at Brule. There were twelve Landsat 8 images that were cloud-free at Brule in 2016. All of these up to September 11 were used in irrigation scheduling. Three more end-of-season images were included in the final analysis. There were seven cloud-free Landsat images over the north half of the Mead field in 2015. There were seven cloud-free images in 2016 and only the first four, up to June 27 and the last one on October 9, included the south half of the field. For the soybean in 2016, there were cloud-free Landsat 7 images on August 22 and September 23, 2016.

3.3. Total prescribed irrigation

Total gross prescribed irrigation was computed as the sum of prescribed irrigation for all irrigation events (**Table 3**). All study plots were included in the prescribed irrigation comparisons. For the 2016 maize, the VRI-NP and uniform treatments had identical irrigation prescriptions. Both ended up being uniform with a total seasonal prescription of 20.3 mm. This was the minimum applied depth (5.08 mm) times the four irrigation events. Essentially, neither of these treatments called for irrigation. Thus the mean, standard error, and confidence interval for VRI-RS for 2016 maize at Mead were computed using PROC MEANS as was done for Brule. Interestingly, for Mead maize in 2016, all variability in irrigation for the VRI-RS treatment was applied in the first irrigation. Thereafter, all subsequent irrigations were uniform applications of the maximum depth allowed for the irrigation protocol (30.45 mm).

The treatment differences between the two VRI treatments were found to be significantly different than zero, at the 5% level, for 2015 maize (standard error of the difference=2.73 mm, $F=295$, $p\text{-value} < 0.0001$) and 2016 soybean (standard error of the difference= 3.35 mm, $F=341$, $p\text{-value} < 0.0001$). The least-squares means for the two VRI treatments are presented in Table 3 with 95% confidence intervals. For the treatments for which confidence intervals were computed, the intervals did not include the mean irrigation depths for any other treatment. Estimated mean irrigation did not exceed 118 mm for any of the Mead treatments. Large amounts of precipitation and low ET were suspected to be the primary drivers of the relatively small amounts of irrigation.

In all cases, the VRI-RS resulted in the greatest irrigation (Table 3) because of overestimation of soil water depletion. Overestimation of ET, DP (D.L. Martin, personal communication), and/or runoff may have been the cause(s) of the soil water balance drift, since the VRI-RS water balance

Table 3. Summary of Mean Total Prescribed Irrigation for the Treatments.

<i>Treatment^a</i>	<i>Mean^b</i> (mm)	<i>SE^c</i> (mm)	<i>df</i>	<i>95% Confidence Interval^d</i>	
				<i>Lower Bound</i>	<i>Upper Bound</i>
Mead Maize 2015					
VRI-RS	86.1	1.9	32	82.1	90.0
VRI-NP	39.3	1.9	32	35.3	43.2
Uniform	45.7				
Mead Maize 2016					
VRI-RS	117.9	2.2	–	112.9	123.0
VRI-NP	20.3				
Uniform	20.3				
Mead Soybean 2016					
VRI-RS	85.8	2.4	32	81.0	90.6
VRI-NP	24.0	2.4	32	19.1	28.8
Uniform	35.6				
Brule Maize 2016					
VRI-RS	342.7	3.1	–	336.0	349.3
Uniform	324.4				

a. Treatment abbreviations were: variable rate irrigation with the remote sensing model (VRI-RS), VRI with neutron probe soil water content (VRI-NP), uniform irrigation (uniform). The rainfed treatment was not prescribed irrigation.

b. Means for VRI-RS and VRI-NP for Mead maize 2015 and soybean 2016 are least-squares means computed using the PROC GLIMMIX. Means, etc. for VRI-RS for both Brule and Mead maize 2016 were computed using PROC MEANS. All other means are uniform values prescribed to all plots in the treatment.

c. Standard error of the means.

d. Confidence intervals of the means.

was not updated with neutron probe data. Overestimation of ET was suspected in 2015, and in 2016 the overestimation of depletion persisted despite modifications to the model. While overestimation of runoff was possible, computed runoff used in all final analyses was about 36 mm for maize in 2015 at Mead; 43 and 44 mm for maize and soybean at Mead in 2016, respectively; and 23mm for maize at Brule in 2016. These magnitudes do not account for the full discrepancy in irrigation between treatments (Table 3), except in the case of Brule.

While the hybrid methodology (Neale et al., 2012) was employed in the VRI-RS in 2016, it apparently did not improve the performance of that treatment. At Mead, the hybrid functionality did not result in soil water depletion adjustments during the experiment since neither the K_{cbrf} nor the TSEB models computed water stress conditions. In the methodology employed in the field study, water-balance-modeled ET_{cfr} was not

adjusted if no adjustment was needed to K_s . Thus, both years at Mead were essentially reliant on the accuracy of the K_{cbrf} and water balance methods. This was not the case at Brule; where the TSEB ET did cause an adjustment in the water balance at times. However, the model still seemed to drift from neutron probe measurements. It seems that ET_{crf} , DP, or runoff may have been overestimated at Brule as well. Uncertainty in FC and WP at Brule likely also contributed to difficulties in both treatments.

The VRI-NP treatment, which approaches an ideal condition for VRI management, had the smallest mean prescribed irrigation of the irrigated treatments at Mead except for maize in 2016 (Table 3). The smaller mean prescribed irrigation for the VRI-NP treatment was evidence that the VRI-NP did effectively manage for some of the spatial variability in the field. This was evidenced by examining the standard deviation of the total prescribed irrigation for a given site-year versus the standard deviation of any single event. This was not a rigorous test, but, it may be evidence that the prescribed irrigation in VRI treatments was not oscillating. For example, if a large irrigation was prescribed to a given plot on one event, irrigation was not necessarily light on the same plot later on. The variation in total prescribed irrigation between plots would possibly be dampened in this case. Similar observations were made for the VRI-RS treatment.

3.4. Response variable MANOVAs and univariate ANOVAs

Treatment effects on response variables were first tested using Wilks' lambda for the Type III sums of squares and cross-products. We failed to reject the null hypothesis that treatment effects were zero at the 5% significance level for 2016 maize at Brule (approximate $F=1.8$, p -value=0.191). This null hypothesis was rejected for all Mead site-years. Blocking effects were found to be significant at the 5% level for Mead soybean in 2016 (approximate $F=3.7$, p -value=0.001). Similarly blocking effects were significant for Mead maize in 2016 (approximate $F=2.3$, p -value=0.036). These are interesting results because they suggests differences induced by soil properties, as represented by EC_a , at Mead in 2016 (blocking was not found to be significant for 2015). The AWC blocking was expected to have a significant effect at Brule, but such was not found at the 5% level (approximate $F=1.8$, p -value=0.065). The span blocking at Brule was also not found to be significant (approximate $F=1.0$, p -value=0.471), though it was anticipated to be so. This was because of visible edge effects in the satellite imagery at Brule. Some of the edge effects

were probably due to the non-irrigated surroundings around the field. The resolution of the Landsat 8 Thermal Infrared Sensor (100 m; Rocchio, 2018) is also acknowledged as a likely cause of edge effects as discussed for some satellites by Gowda et al. (2007).

The univariate ANOVAs were examined for all of the Mead site-years, but not for Brule because of the MANOVA results (Table 4). Of all of the univariate ANOVA analyses, the null hypotheses that at least one of the treatments had an estimated mean that differed from the others were rejected at the 5% level for all but three cases. These cases were DP in 2016 soybean and maize at Mead and yield for 2016 maize at Mead ($F=1.38$, $p\text{-value}=0.26$; $F=1.22$, $p\text{-value}=0.32$; and $F=1.17$, $p\text{-value}=0.34$, respectively).

3.5. Yield and water use efficiency

As mentioned in 2.6, the yield response estimates were obtained from harvest combine yield maps. All yields reported here are at harvest moisture contents. In 2015, the average maize yield was 13.1 Mg ha^{-1} based on weighing grain cart data, which had moisture contents of 13.7%–14.6%, with an effective mean of 14.1%. The field-average yield from the cleaned yield map was computed by Yield Editor to be 13.2 Mg ha^{-1} with an effective mean moisture content of 13.9% from the yield monitor data. In 2016, the grain cart field-average maize yield was 13.4 Mg ha^{-1} with moisture contents of 15.7%–16.5%, with an effective mean of 16.1%. The yield map average was 13.7 Mg ha^{-1} with an effective moisture content of 16.0% from the yield monitor data. This was a difference of about 2%. For soybean in 2016, the field total and yield map average yields were both 4.3 Mg ha^{-1} . The moisture contents from the grain cart data were 12.4%–14.4%, with an effective mean of 13.0%. The effective mean moisture content from the yield monitor data was 12.6%. No further adjustment or scaling was applied to the yield estimates because they were near the grain cart averages. For Brule, the cleaned maize yield was about 9.7 Mg ha^{-1} with an effective moisture content from the yield monitor data of 14.3% for the processed parts of the field. We only processed the yield for the study plots at Brule, so a comparison with total field yield was not performed.

Estimated least-squares means for yield and other response variables are presented in **Table 4**. For yield in the 2015 maize, the two VRI treatments and the rainfed treatment all had similar estimated means (13.3 Mg ha^{-1}); they were only found to be significantly different than the

Table 4. Estimated Least-Squares Means from Univariate ANOVAs.

Response Variable ^a	Treatment ^b Least-Squares Mean (Standard Error) ^c			
	VRI-RS	VRI-NP	Uniform	Rainfed
ARDC Maize 2015				
Yield (Mg ha ⁻¹)	13.3 (0.11)-A	13.3 (0.09)-A	12.9 (0.09)-B	13.3 (0.10)-A
ET _a (mm)	413 (4.5)-A	374 (3.9)-B	373 (3.9)-B	343 (4.2)-C
P-RO+Inet+ΔSW (mm)	413 (4.5)-A	374 (3.9)-B	373 (3.9)-B	343 (4.2)-C
DP (mm) ^d	0 (-)	0(-)	0(-)	0(-)
ARDC Maize 2016				
Yield (Mg ha ⁻¹)	14.1 (0.25)	13.9 (0.29)	13.8 (0.23)	13.4 (0.25)
ET _a (mm)	492 (7.4)-A	413 (8.6)-BC	421 (6.9)-B	393 (7.4)-C
P-RO+Inet+ΔSW (mm)	493 (5.3)-A	426 (6.1)-B	425 (4.9)-B	397 (5.3)-C
DP (mm)	1 (4.4)	13 (5.1)	3 (4.1)	4 (4.4)
ARDC Soybean 2016				
Yield (Mg ha ⁻¹)	4.2 (0.05)-B	4.4 (0.05)-AB	4.3 (0.05)-AB	4.5 (0.04)-A
ET _a (mm)	512 (6.9)-A	468 (6.9)-B	465 (6.9)-B	452 (6.0)-B
P-RO+Inet+ΔSW (mm)	521 (5.8)-A	470 (5.8)-B	470 (5.8)-B	455 (5.0)-B
DP (mm)	9 (2.7)	1 (2.7)	5 (2.7)	3 (2.3)
Brule Maize 2016				
Yield (Mg ha ⁻¹)	10.2 (0.32)	–	10.0 (0.32)	–
ET _a (mm)	412 (11.1)	–	408 (11.3)	–
P-RO+Inet+ΔSW (mm)	425 (5.4)	–	413 (5.5)	–
DP (mm)	13 (7.4)	–	5 (7.5)	–

a. Response variable abbreviations were: measurement period actual evapotranspiration (ET_a), measurement period precipitation – estimated runoff + net prescribed irrigation + change in measured soil water content (P-RO+Inet+ΔSW), and measurement period estimated deep percolation (DP).

b. Treatments were: variable rate irrigation with the remote sensing model (VRI-RS), VRI with neutron probe soil water measurement (VRI-NP), uniform irrigation (uniform), and rainfed.

c. Treatment means were not found to be significantly different at the 5% level, using a Tukey-Kramer adjustment, for a given single variable in a given crop-year if they share the same grouping letter. If no grouping letters are presented, then treatment effects were not found to be significant.

d. DP was estimated to be zero for all plots in 2015.

uniform treatment (12.9 Mg ha⁻¹). These differences were unlikely to be strictly a response to the irrigation treatment and were attributed to random error. For 2016 maize at Mead, the range in yield was 13.4–14.1 Mg ha⁻¹ for rainfed and VRI-RS, respectively. Treatment differences were not significantly different. For 2016 soybean, the estimated mean yield in the rainfed treatment was the greatest (4.5 Mg ha⁻¹); this was only found to be significantly different than the VRI-RS treatment (4.2 Mg ha⁻¹). The larger estimated mean yield for the rainfed treatment over the VRI-RS treatment for the soybean may be a result of soybean not having

improved yield from increased irrigation. This is a known effect, as a result of plant lodging from excessive vegetative growth (Kranz and Specht, 2012). Soybean lodging was observed throughout the field in 2016. Irrigation water use efficiency was estimated using the yield estimates from Table 4 and the corresponding mean prescribed irrigation (excluding the same plots as for the response variables). As the method for computing means was different for some of the irrigation treatments, simple means of both yield and irrigation using PROC MEANS were also used in computing water use efficiency (shown in parenthesis). For 2015 maize, irrigation water use efficiency ranged from -8.3 (-8.4) $\text{kg ha}^{-1}\text{mm}^{-1}$ for the uniform treatment to 1.0 (0.9) $\text{kg ha}^{-1}\text{mm}^{-1}$ for the VRI-NP. The VRI-RS was less than -0.1 (-0.02) $\text{kg ha}^{-1}\text{mm}^{-1}$. For 2016 maize at Mead, irrigation water use efficiency ranged from 5.5 (5.0) $\text{kg ha}^{-1}\text{mm}^{-1}$ for the VRI-RS treatment to 22.7 (17.8) $\text{kg ha}^{-1}\text{mm}^{-1}$ for the VRI-NP, with 18.6 (17.4) $\text{kg ha}^{-1}\text{mm}^{-1}$ for the uniform. Note that for this site-year, VRI-RS was computed as a simple mean over plots included in the response variable ANOVAs for that site-year. All irrigation water use efficiencies were negative for the soybean possibly due to yield losses associated with lodging (Rudnick et al., 2016). Efficiencies were -5.1 (-5.1) $\text{kg ha}^{-1}\text{mm}^{-1}$ for VRI-NP, -3.6 (-3.7) $\text{kg ha}^{-1}\text{mm}^{-1}$ for uniform, and -3.0 (-3.0) $\text{kg ha}^{-1}\text{mm}^{-1}$ for VRI-RS. Efficiencies were not computed for Brule due to the lack of a rainfed treatment. Longer-term experiments including dry years would provide a better perspective on how much VRI can increase irrigation water use efficiency.

3.6. Hydrologic response variables

While the reported ET_a values (Table 4) appear to be low for all site-years, it should be emphasized that they are for the measurement periods, not the full growing seasons. Neutron probe measurements began 21–38 days after planting; therefore an appreciable amount of evapotranspiration is likely not accounted for in the estimated means presented in Table 4. In general, treatments were expected to be similar, although some differences in ET_a were expected due to increased wet soil evaporation from irrigation.

For maize in 2015, the VRI-RS had the greatest estimated mean ET_a (413 mm). This was significantly different than all other treatments, with the lowest being rainfed (343 mm). This difference (70 mm) seems excessive considering the various irrigation treatments were applied after tasseling. A similar observation was made for Mead maize in 2016, with the VRI-RS treatment having the greatest ET_a (492 mm). This response was

Table 5. Coefficients of Variation for Response Variables, Precipitation, and Available Water Capacity for the Uniform Treatment in the Different Site-Years.

Variable ^a	ARDC Maize		Soybean	Brule Maize	Average Coefficient of Variation
	2015	2016	2016	2016	
Count	18	8	13	14	
	—————Coefficient of Variation (%)—————				
Yield	3.1	6.6	5.1	10.8	6.4
AWC	9.5	6.3	9.7	24.8	12.6
Precipitation ^b	6.7	8.7	8.7	–	7.7
P-RO+I _{net} +ΔSW	5.0	6.2	5.0	4.8	5.2
DP	– ^c	194	222	283	233
ET _a	5.0	6.8	5.6	8.8	6.5

- a. Variable abbreviations are: available water content (AWC), measurement period precipitation–estimated runoff+net prescribed irrigation+change in measured soil water content (P-RO+I_{net}+ΔSW), estimated measurement period deep percolation (DP), and measurement period estimated actual evapotranspiration (ET_a). Variation in precipitation is computed between the four rain gauges at Mead.
- b. The coefficient of variation for precipitation in 2016 was not double counted in the reported average.
- c. Estimated DP was zero for all plots in 2015.

found to be significantly different than all other treatments. Again, the lowest ET_a was rainfed (393 mm). This difference (99 mm) seems excessive given that the first irrigation was started on July 15, 2016. For the soybean at Mead in 2016, ET_a was greatest for the VRI-RS (512 mm), which was significantly different than the other treatments, with the smallest again being rainfed (452 mm). This was a 60mm difference in estimated means. Differences in ET_a for maize at Brule were not significant, and had a smaller range of about 4 mm.

The large differences in estimated mean ET_a for individual crop-years at Mead may be related to uncertainty in the DP computation method. Possible improvements to estimating DP could include using multiple layer soil water balances (Djaman and Irmak, 2012), a more physically-based approach such as the Wilcox method (Klocke et al., 2010; Miller and Aarstad, 1972), or possibly even inverse modeling (Foolad et al., 2017). Such methods may better account for spatial variability in drainage rates.

The uncertainties in ET_a computations support the inclusion of DP and of P-RO+I_{net}+ΔSW as a combined variable. For Mead maize, significant differences in P-RO+I_{net}+ΔSW were similar to ET_a, with ranges of 70 mm

for 2015 and 96 mm for 2016. Both were within 20 mm of prescribed irrigation, suggesting that this variable accounted for the change in the water balance due to irrigation. If all processes were exactly accounted for, the differences in $P-RO+I_{net}+\Delta SW$ should be equal to differences in net irrigation. For soybean, estimated mean $P-RO+I_{net}+\Delta SW$ was greatest for the VRI-RS treatment (521 mm), which is logical. This was significantly different than all other treatments, with the smallest being 455 mm for rainfed. Again, this difference was within 20mm of the difference in prescribed irrigation.

Estimated DP in the final analysis was lower than estimated DP during irrigation scheduling (see 2.6). No significant differences between treatments were found in DP. Deep percolation was estimated to be 0 for all plots in 2015. For 2016 maize and soybean at Mead, DP was estimated to be 13 mm or less and 9 mm or less, respectively. Allowing drainage to occur over the course of multiple days resulted in little DP being estimated. Deep percolation was estimated to be 13 mm or less for Brule.

3.7. Spatial variability

We investigated the spatial variability of the three primary response variables (yield, ET_a , DP, and $P-RO+I_{net}+\Delta SW$), precipitation, and AWC to identify which variables were most important to quantify spatially for irrigation management. Only the uniform treatment was included for this purpose. This treatment had no intentionally imposed variability and was included for all site-years. To compare spatial variability, the coefficient of variation (CV) was computed for each variable using Microsoft Excel (Table 5), without accounting for blocking or other treatments. Missing data from some blocks were acknowledged, but were not accounted for in this analysis. Spatial variability in precipitation was computed for the cumulative precipitation from each of four rain gauges at Mead. The period of June 26 to July 15 and September 9 to October 14, 2015 and the period of June 9 through September 13, 2016 were used for precipitation. Another potential driving force for spatial differences in irrigation requirements is run-on within the field; however, this effect was not quantified in the analysis.

For all cases except 2015, DP had the largest CV, which is primarily due to the low magnitude of the estimates. (Deep percolation was computed to be zero for all plots in 2015.) The following discussion subsequently ignores DP. A better measure of the variability may likely be gleaned by examining CVs for ET_a and $P-RO+I_{net}+\Delta SW$. For 2015 at Mead, the greatest variability as defined by the CV was in AWC, followed by precipitation. For

2016 at Mead, the greatest variability was in AWC for the soybean and precipitation for the maize. Overall, the AWC, precipitation and ET_a had greater variability than did yield at Mead (though the CV for AWC was less than for yield for 2016 maize), suggesting a dampened response of yield to the soil and ET_a variability. At Brule, AWC had the greatest variability, which was much larger than at Mead. Part of this difference was related to the smaller mean AWC at Brule, but greater variation was expected at that site due to great soil heterogeneity. From Table 5, it seems that quantifying AWC may be most important for VRI management followed by precipitation and ET (assuming that the CV presented here is representative of the CV of actual ET).

4. Conclusions

The VRI-RS treatment had the greatest mean prescribed irrigation for each crop-year combination. The differences were attributed to water balance drift. Even after model improvements were made in 2016, the drift was still apparent. Overestimation of wet soil evaporation, drainage rates, and/or runoff are suspected as contributing causes of the drift. In the final analyses, soil evaporation was dampened by 25% based on residue estimates at Mead and DP was limited to not occur until it had been more than three days since a rainfall or irrigation event at Mead and more than one day later for Brule in final analyses (D.L. Martin, personal communication). Further improvements to these parts of the model is recommended. The remote-sensing-based model is expected to perform better if coupled with soil water content measurement.

Treatment effects were primarily in ET_a or $P-RO+I_{net}+\Delta SW$, with increased irrigation generally resulting in greater estimates of both. Yield differences were small; yield differences in maize may have resulted from random error. Yield reductions in soybean for the VRI-RS treatment may have been a result of lodging caused by excess irrigation (Kranz and Specht, 2012).

Of the variables considered in this research, AWC generally had the greatest spatial variability, more so than ET_a or $P-RO+I_{net}+\Delta SW$. However, these were still variable, and precipitation had the greatest variability for 2016 maize at Mead (excluding DP). Thus quantifying spatial variability beyond AWC may improve irrigation management.

The small number of cloud-free satellite images was a challenge for properly executing the remote-sensing-based model. However, the provisions for real-time operation performed well given the number of input

images. It is expected that the hybrid functionality of the model would perform better in environments where water stress was more likely to be encountered.

Acknowledgments — Funding for the project was provided through the Robert B. Daugherty Water for Food Global Institute at the University of Nebraska and the Agricultural Research Division, University of Nebraska-Lincoln. This project was also partially supported by the Nebraska Agricultural Experiment Station with funding from the Hatch Act (Accession Number 1009760), and an Agricultural and Food Research Initiative grant (Award Number 2017-67021-26249), both through the USDA National Institute of Food and Agriculture. Barker was supported, in part, by a University of Nebraska Presidential Fellowship. We thank Mr. Mark Schroeder, Facilities Director of the University of Nebraska Eastern Nebraska Research and Extension Center, and others at that facility for their support of this research including provision of yield data. We thank personnel at the University of Nebraska-Lincoln West Central Research and Extension Center for providing data and field support for the Brule site. We are grateful for those who helped with data collection, laboratory work, field operations, equipment, facilities, and/or advisory input, especially Tsz Him Lo. Others include: Raoni Bosquilla, Clayton Blagburn, Alan Boldt, Isidro Campos, Blaine Clowser, Roger Elmore, Ryan Freiburger, Tomie Galusha, Isaiah Krutak, Rodrigo Dal Sasso Lourenço, Keith Miller, Mumba Mwape, Christopher Proctor, Matthew Russell, Aaron Steckly, Keith Stewart, and Christian Uwineza. Dr. Joe Luck provided the electrical conductivity data and advise on EC_a and yield processing for Mead. Dr. Trenton Franz provided the interpolated electrical conductivity data for Brule. The Nebraska Mesonet weather data were provided by the High Plains Regional Climate Center at the University of Nebraska-Lincoln. The Ogallala AWOS weather station data were provided by the Utah Climate Center. Landsat imagery including surface reflectance “data available from the U.S. Geological Survey” (<https://lta.cr.usgs.gov/citation>). We thank Dr. Kent Eskridge and the University of Nebraska-Lincoln Statistical Crossdisciplinary Collaboration and Consulting Lab, who provided statistical support. We thank Drs. Derrel Martin, William Kranz, Trenton Franz, and Kent Eskridge, and Ms. Ronica Stromberg, for their reviews of earlier versions of this manuscript. We also thank the anonymous reviewers for their input.

References

- Allen, R.G., Pereira, L.S., Raes, D., Smith, M., 1998. Crop evapotranspiration: guidelines for computing crop water requirements. Irrigation and Drainage Paper 56. Food and Agriculture Organization of the United Nations, Rome, Italy.
- Allen, R.G., Wright, J.L., 1997. Translating wind measurements from weather stations to agricultural crops. *J. Hydrol. Eng.* 2, 26–35. doi 10.1061/(ASCE)1084-0699(1997)2:1(26)

- Allen, R.G., Wright, J.L., 2002. Conversion of Wright (1981) and Wright (1982) Alfalfa-based Crop Coefficients for Use with the ASCE Standardized Penman-Monteith Reference Evapotranspiration Equation. Retrieved From https://www.kimberly.uidaho.edu/water/asceewri/Conversion_of_Wright_Kcs_2c.pdf (October 4, 2017).
- Anderson, M.C., Neale, C.M.U., Li, F., Norman, J.M., Kustas, W.P., Jayanthi, H., Chavez, J.L., 2004. Upscaling ground observations of vegetation water content, canopy height, and leaf area index during SMEX02 using aircraft and Landsat imagery. *Remote Sens. Environ.* 92, 447–464. doi 10.1016/j.rse.2004.03.019
- ASCE-EWRI, 2005. ASCE Standardized Reference Evapotranspiration Equation. In: Allen, R.G., Walter, I.A., Elliott, R.L., Howel, T.A., Itenfisu, D., Jensen, M.E. (Eds.), Task Committee on Standardization of Reference Evapotranspiration. Environmental and Water Resources Institute of the American Society of Civil Engineers, Reston, VA. Retrieved from <https://www.kimberly.uidaho.edu/water-asceewri/ascestzdetmain2005.pdf> and <http://www.kimberly.uidaho.edu/water/asceewri/appendix.pdf>
- Barker, J.B., 2017. Spatial Irrigation Management Using Remote Sensing Water Balance Modeling and Soil Water Content Monitoring. Biological Systems Engineering Department. University of Nebraska-Lincoln, Lincoln, NE.
- Barker, J.B., Franz, T.E., Heeren, D.M., Neale, C.M.U., Luck, J.D., 2017. Soil water content monitoring for irrigation management: a geostatistical analysis. *Agric. Water Manage.* 188, 36–49. doi 10.1016/j.agwat.2017.03.024
- Barker, J.B., Heeren, D.M., Neale, C.M.U., 2016. Perspectives on VRI prescription map development with satellite imagery. In: 28th Annual Central Plains Irrigation Conference and Exposition Proceedings, February 23–24, 2016 Central Plains Irrigation Association, Colby, KS. Kearney, NE., pp. 59–67.
- Barker, J.B., Neale, C.M.U., Heeren, D.M., Suyker, A.E., 2018. Evaluation of a hybrid reflectance-based crop coefficient and energy balance evapotranspiration model for irrigation management. *Trans. ASABE*. doi 10.13031/trans.12311. (in press).
- Barsi, J., Atmospheric Correction Parameter Calculator. National Aeronautics and Space Administration, no date. <https://atmcorr.gsfc.nasa.gov/> (September 21, 2017).
- Bausch, W.C., 1993. Soil background effects on reflectance-based crop coefficients for corn. *Remote Sens. Environ.* 46, 213–222. doi 10.1016/0034-4257(93)90096-g
- Bausch, W.C., Neale, C.M.U., 1987. Crop coefficients derived from reflected canopy radiation – a concept. *Trans. ASAE* 30, 703–709. doi 10.13031/2013.30463.
- Brady, N.C., Weil, R.R., 1996. *The Nature and Properties of Soils*, 11th ed. Prentice-Hall Inc., Upper Saddle River, NJ.
- Brunsell, N.A., Gillies, R.R., 2002. Incorporating surface emissivity into a thermal atmospheric correction. *Photogramm. Eng. Remote Sens.* 68, 1263–1269.

- Campos, I., Neale, C.M.U., Suyker, A.E., Arkebauer, T.J., Gonçalves, I.Z., 2017. Reflectance-based crop coefficients redux: for operational evapotranspiration estimates in the age of high producing hybrid varieties. *Agric. Water Manage.* 187, 140–153. doi 10.1016/j.agwat.2017.03.022
- Colaizzi, P.D., Agam, N., Tolk, J.A., Evett, S.R., Howell, T.A., Gowda, P.H., O’Shaughnessy, S.A., Kustas, W.P., Anderson, M.C., 2014. Two-source energy balance model to calculate E, T, and ET: comparison of Priestley-Taylor and Penman-Monteith formulations and two time scaling methods. *Trans. ASABE* 57, 479–498. doi 10.13031/trans.57.10423
- Djaman, K., Irmak, S., 2012. Soil water extraction patterns and crop, irrigation, and evapotranspiration water use efficiency of maize under full and limited irrigation and rainfed settings. *Trans. ASABE* 55. doi 10.13031/2013.42262
- Foolad, F., Franz, T.E., Wang, T., Gibson, J., Kilic, A., Allen, R.G., Suyker, A., 2017. Feasibility analysis of using inverse modeling for estimating field-scale evapotranspiration in maize and soybean fields from soil water content monitoring networks. *Hydrol. Earth Syst. Sci.* 21, 1263–1277. doi 10.5194/hess-21-1263-2017
- Geli, H.M.E., 2012. Modeling Spatial Surface Energy Fluxes of Agricultural and Riparian Vegetation Using Remote Sensing. Civil and Environmental Engineering Department. Utah State University, Logan, UT.
- Geli, H.M.E., Lewis, C.S., Contributors, 2014. SETMI (ca. November 5, 2014). [Source Code]. Utah State University, Logan, UT.
- Geli, H.M.E., Neale, C.M.U., 2012. Spatial evapo transpiration modelling interface (SETMI). In: Neale, C.M.U., Cosh, M.H. (Eds.), *Remote sensing and hydrology (proceedings of a symposium held at Jackson Hole, Wyoming, USA, September 2010)* Publ. 352. International Association of Hydrological Sciences, Wallingford, Oxfordshire, UK. pp. 171–174.
- Gowda, P.H., Chavez, J.L., Colaizzi, P.D., Evett, S.R., Howell, T.A., Tolk, J.A., 2007. Remote sensing based energy balance algorithms for mapping ET: current status and future challenges. *Trans. ASABE* 50, 1639–1644. doi 10.13031/2013. 23964.
- Higgins, C.W., Kelley, J., Barr, C., Hillyer, C., 2016. Determining the minimum management scale of a commercial variable-rate irrigation system. *Trans. ASABE* 59, 1671–1680. doi 10.13031/trans.59.11767
- Howell, T.A., 2001. Enhancing water use efficiency in irrigated agriculture. *Agron. J.* 93, 281–289. doi 10.2134/agronj2001.932281x
- HPRCC, 2018. Active NE AWDN Stations. Automated Weather Data Network. High Plains Regional Climate Center, University of Nebraska-Lincoln, Lincoln, NE. http://awdn.unl.edu/total_numbered.txt (February 27, 2018).
- Huete, A.R., 1988. A soil-adjusted vegetation index (SAVI). *Remote Sens. Environ.* 25, 295–309. doi 10.1016/0034-4257(88)90106-x
- Irmak, S., Specht, J.E., Odhiambo, L.O., Rees, J.M., Cassman, K.G., 2014. Soybean yield, evapotranspiration, water productivity, and soil water extraction response to subsurface drip irrigation and fertigation. *Trans. ASABE* 57, 729–748. doi 10.13031/trans.57.10085

- Jensen, M.E., Allen, R.G., 2016. Evaporation, Evapotranspiration, and Irrigation Water Requirements, ASCE Manuals and Reports on Engineering Practice No. 70. 2nd ed. American Society of Civil Engineers, Reston, VA.
- Klocke, N.L., Stone, L.R., Briggeman, S., Bolton, D.A., 2010. Technical note: scheduling for deficit irrigation—crop yield predictor. *Appl. Eng. Agric.* 26, 413–418. doi 10.13031/2013.29956
- Kranz, W.L., Specht, J.E., 2012. Irrigating Soybean, NebGuide G1367. Rev. December 2012. University of Nebraska–Lincoln Extension, Institute of Agriculture and Natural Resources University of Nebraska–Lincoln, Lincoln, NE. Available at: <http://extensionpubs.unl.edu/publication/9000016368734/irrigating-soybean/>
- Li, F.Q., Kustas, W.P., Prueger, J.H., Neale, C.M.U., Jackson, T.J., 2005. Utility of remote sensing-based two-source energy balance model under low- and high-vegetation cover conditions. *J. Hydrometeorol.* 6, 878–891. doi 10.1175/jhm464.1
- Lo, T.H., Heeren, D.M., Martin, D.L., Mateos, L., Luck, J.D., Eisenhauer, D.E., 2016. Pumpage reduction by using variable-rate irrigation to mine undepleted soil water. *Trans. ASABE* 59, 1285–1298. doi 10.13031/trans.59.11773.
- Lo, T.H., Heeren, D.M., Mateos, L., Luck, J.D., Martin, D.L., Miller, K.A., Barker, J.B., Shaver, T.M., 2017. Field characterization of field capacity and root zone available water capacity for variable rate irrigation. *Appl. Eng. Agric.* 33 (4), 559–572. <http://dx.doi.org/10.13031/aea.11963>
- Martin, D.L., Stegman, E.C., Fereres, E., 1990. Irrigation scheduling principles. In: Hoffman, G.J., Howell, T.A., Solomon, K.H. (Eds.), *Management of Farm Irrigation Systems*, ASAE Monograph No. 9. American Society of Agricultural Engineers, St. Joseph, MI, pp. 155–203.
- Merriam, J.L., 1966. A management control concept for determining the economical depth and frequency of irrigation. *Trans. ASAE* 9, 492–498. doi 10.13031/2013.40014
- Miller, D.E., Aarstad, J.S., 1972. Estimating deep drainage between irrigations. *Soil Sci. Soc. Am. J.* 36, 124–127. doi 10.2136/sssaj1972.03615995003600010029x.
- NCEI, Data Tools: 1981–2010 Normals. National Oceanic and Atmospheric Administration National Centers for Environmental Information, no date. <http://www.ncdc.noaa.gov/cdo-web/datatools/normals> (May 8, 2017).
- Neale, C.M.U., Bausch, W.C., Heermann, D.F., 1989. Development of reflectance-based crop coefficients for corn. *Trans. ASAE* 32, 1891–1899. doi 10.13031/2013.31240
- Neale, C.M.U., Geli, H.M.E., Kustas, W.P., Alfieri, J.G., Gowda, P.H., Evett, S.R., Prueger, J.H., Hipps, L.E., Dulaney, W.P., Chavez, J.L., French, A.N., Howell, T.A., 2012. Soil water content estimation using a remote sensing based hybrid evapotranspiration modeling approach. *Adv. Water Resour.* 50, 152–161. doi 10.1016/j.advwatres.2012.10.008.
- Norman, J.M., Kustas, W.P., Humes, K.S., 1995. A two-source approach for estimating soil and vegetation energy fluxes in observations of directional radiometric surface temperature. *Agric. For. Meteorol.* 77, 263–293. doi 10.1016/0168-1923(95)02265-y

- NWS, Station Pressure. U.S. Department of Commerce National Oceanic and Atmospheric Administration National Weather Service, Salt Lake City, UT, no date. Retrieved from <http://www.wrh.noaa.gov/slc/projects/wxcalc/formulas/pressureAltitude.pdf> (September 3, 2015)
- Odhiambo, L.O., Irmak, S., 2012. Evaluation of the impact of surface residue cover on single and dual crop coefficient for estimating soybean actual evapotranspiration. *Agric. Water Manage.* 104, 221–234. doi 10.1016/j.agwat.2011.12.021.
- Rocchio, L., 2018. Landsat 8. Landsat Science. National Aeronautics and Space Administration. Last Updated February 26, 2018. <https://landsat.gsfc.nasa.gov/landsat-data-continuity-mission/> (February 28, 2018).
- Rouse, J.W., Haas, R.H., Schell, J.A., Deering, D.W., Harlan, J.C., 1974. Monitoring the Vernal Advancement and Retrogradation (Greenwave Effect) of Natural Vegetation. Texas A & M University, Remote Sensing Center, College Station, TX.
- Rudnick, D., Irmak, S., Ferguson, R., Shaver, T., Djaman, K., Slater, G., Bereuter, A., Ward, N., Francis, D., Schmer, M., Wienhold, B., Donk, S.V., 2016. Economic return versus crop water productivity of maize for various nitrogen rates under full irrigation, limited irrigation, and rainfed settings in South Central Nebraska. *J. Irrig. Drain. Eng.* 142, 04016017. doi 10.1061/(ASCE)IR.1943-4774.0001023
- Shelton, D.P., Jasa, P.J., 2009. Estimating Percent Residue Cover Using the Line-Transect Method, NebGuide G1931. University of Nebraska-Lincoln Extension, Institute of Agriculture and Natural Resources, University of Nebraska-Lincoln, Lincoln, NE. Available at: <http://extensionpubs.unl.edu/publication/9000016366649/estimating-percent-residue-cover-using-the-line-transect-method/>
- Soil Survey Staff, 2016a. Web Soil Survey. U.S. Department of Agriculture Natural Resources Conservation Service. Available at: <http://websoilsurvey.sc.egov.usda.gov> (February 23, 2017).
- Soil Survey Staff, 2016b. Web Soil Survey. U.S. Department of Agriculture Natural Resources Conservation Service. Available at: <http://websoilsurvey.sc.egov.usda.gov> (September 8, 2016).
- Stone, K.C., Bauer, P.J., Sigua, G.C., 2016. Irrigation management using an expert system, soil water potentials, and vegetative indices for spatial applications. *Trans. ASABE* 59, 941–948. doi 10.13031/trans.59.11550
- Sudduth, K.A., Drummond, S.T., Myers, D.B., 2012. Yield editor 2.0: software for automated removal of yield map errors, ASABE Paper No. 12-1338240. In: 2012 ASABE Annual International Meeting, Dallas, TX, 29 July 29 - August 1, 2012. American Society of Agricultural and Biological Engineers. pp. 1–14. St. Joseph, MI. doi 10.13031/2013.41893.
- Sudduth, K.A., Kitchen, N.R., Wiebold, W.J., Batchelor, W.D., Bollero, G.A., Bullock, D.G., Clay, D.E., Palm, H.L., Pierce, F.J., Schuler, R.T., Thelen, K.D., 2005. Relating apparent electrical conductivity to soil properties across the north-central USA. *Comput. Electron. Agric.* 46, 263–283. doi 10.1016/j.compag.2004.11.010
- USBR, 2016, About AgriMet Crop Coefficients. U.S. Department of the Interior Bureau of Reclamation Pacific Northwest Region AgriMet; Boise, ID, Last updated January 28, 2016, https://www.usbr.gov/pn/agrimet/cropcurves/about_crop_curves.html (February 28 2018).

- USDA-FSA, 2012. USDA-FSA-APFO NAIP MrSID Mosaic for Saunders County, Nebraska. U.S. Department of Agriculture, Service Center Agencies, Farm Service Agency, Aerial Photography Field Office, National Agricultural Imagery Program. Retrieved from <http://datagateway.nrcs.usda.gov/>
- USDA-NRCS, 2004. Chapter 10, estimation of direct runoff from storm rainfall, part 630 hydrology. National Engineering Handbook. U.S. Department of Agriculture, Natural Resources Conservation Service, Washington, D.C. Retrieved from <https://www.wcc.nrcs.usda.gov/ftpref/wntsc/H&H/NEHydrology/ch10.pdf>
- USDA-NRCS, 2009a. Processed TIGER 2002 Counties+NRCS Additions Dissolve. U.S. Department of Agriculture, Service Center Agencies, Natural Resources Conservation Service, National Geospatial Center of Excellence. Retrieved from <http://datagateway.nrcs.usda.gov/>
- USDA-NRCS, 2009b. Processed TIGER 2002 Counties Plus NRCS Additions. U.S. Department of Agriculture, Service Center Agencies, Natural Resources Conservation Service, National Geospatial Center of Excellence. Retrieved from <http://datagateway.nrcs.usda.gov/>
- van Donk, S.J., McGee, A.L., Klopfenstein, T.J., Stalker, L.A., MP95, 2012. Effect of corn stalk grazing and baling on cattle performance and irrigation needs. In: Agricultural Research Division and University of Nebraska Extension (Ed.), 2012 Beef Cattle Report Agricultural Research Division. University of Nebraska-Lincoln Extension, Institute of Agriculture and Natural Resources, University of Nebraska-Lincoln, Lincoln, NE, pp. 8–10. Available at: <https://beef.unl.edu/86f51d68-be05-44ac-87f5-5a5d8dbd9470.pdf>
- Wright, J.L., 1982. New evapotranspiration crop coefficients. *J. Irrig. Drain. Eng. Proc. Am. Soc. Civil Eng.* 108 (IR1), 57–74.
- Yonts, D.C., Melvin, S.R., Eisenhauer, D.E., 2008. Predicting the Last Irrigation of the Season, NebGuide G1871. University of Nebraska-Lincoln Extension, Institute of Agriculture and Natural Resources, University of Nebraska-Lincoln, Lincoln, NE. Available at: <http://extensionpubs.unl.edu/publication/9000016365946/predicting-the-last-irrigation-of-the-season/>
- Zreda, M., Location of COSMOS Probes, no date. Retrieved from: <http://cosmos.hwr.arizona.edu/Probes/probemap.php> (Accessed December 5, 2016).
- Zreda, M., Shuttleworth, W.J., Zeng, X., Zweck, C., Desilets, D., Franz, T.E., Rosolem, R., 2012. COSMOS: the COsmic-ray soil moisture observing system. *Hydrol. Earth Syst. Sci.* 16, 4079–4099. doi 10.5194/hess-16-4079-2012